Published in final edited form as:
J Med Chem. 2008 November 27; 51(22): 7234–7242. doi:10.1021/jm8008585.

Interrogating the Bioactive Pharmacophore of the Latrunculin Chemotype by Investigating the Metabolites of Two Taxonomically Unrelated Sponges

Taro Amagata[†], **Tyler A. Johnson**[†,‡], **Robert H. Cichewicz**[†], **Karen Tenney**[†], **Susan L. Mooberry**[§], **Joseph Media**[⊥], **Matthew Edelstein**[⊥], **Frederick A. Valeriote**[⊥], and **Phillip Crews**[*,†,‡]

Department of Chemistry and Biochemistry and Department of Ocean Sciences, University of California Santa Cruz, Santa Cruz, CA 95064, Southwest Foundation for Biomedical Research, San Antonio, Texas 78245, and Henry Ford Hospital, Department of Internal Medicine, Division of Hematology and Oncology, Detroit, MI 48202

Abstract

This study involved a campaign to isolate and study additional latrunculin analogs from two taxonomically unrelated sponges, *Cacospongia mycofijiensis* and *Negombata magnifica*. A total of 13 latrunculin analogs were obtained by four different ways, reisolation (**1**–**4**), our repository (**5**–**6**), new derivatives (**7**–**12**), and a synthetic analog (**7a**). The structures of the new metabolites were elucidated based on a combination of comprehensive 1D and 2D NMR analysis, application of DFT calculations, and the preparation of acetonide derivative **7a**. The cytotoxicities against both murine and human cancer cell lines observed for **1**, **2**, **7**, **7a**, **8**, **9**, and **12** were significant and the IC_{50} value range was 0.5–10 μM. Among the cytotoxic derivatives, compound **9** did not exhibit microfilament-disrupting activity at 5 μM. The implications of this observation and the value of further therapeutic study on key latrunculin derivatives are discussed.

Introduction

The latrunculins are an important group of sponge-derived bioactive small molecules whose properties have been extensively studied for almost 30 years.[1] The two lead compounds of this series are latrunculin A (**1**) and latrunculin B (**2**), originally isolated from the Red Sea sponge *Negombata magnifica* (old genus designation *Latrunculia*).[1,2] Their basic structural motif consists of a macrolide 1,3 fused to a tetrahydropyran containing a 2-thiazolidinone side chain. Compound **1** also shares a carbon skeleton with the anti-cancer active epothilone A,[3] obtained from cultures of the terrestrial myxobacterium, *Sorangium cellulosum*.[4,5] The sustained attention given to the latrunculins can be attributed to three factors–a unique mixed biogenesis from PKS/NRPS,[a,3] their potent actin inhibition properties,[2,6] and their potent cytotoxicity against cancer cell lines.[7] In comparison to the many other common natural product actin inhibitors[8] latrunculin A is the most widely used small molecule molecular probe. Its actin

*To whom correspondence should be addressed. Tel: (831) 459-2603. Fax: (831) 459-4197. phil@chemistry.ucsc.edu.
[†]Department of Chemistry and Biochemistry, University of California Santa Cruz
[‡]Department of Ocean Sciences, University of California Santa Cruz
[§]Southwest Foundation for Biomedical Research
[⊥]Henry Ford Hospital

Supporting Information Available: Isolation scheme and underwater picture for *N. magnifica* and *C. mycofijiensis*, the NMR data for **1**, **2**, **3**, **4**, **7**, **8**, **9**, **10**, **11** and **12**, the DFT calculations results for **7** and **10**. This material is available free of charge via the Internet at http://pubs.acs.org

inhibition properties result from blocking the hyper-assembly of G-actin to F-actin[6] by binding to a site in a cleft between subdomains II and IV.[9,10]

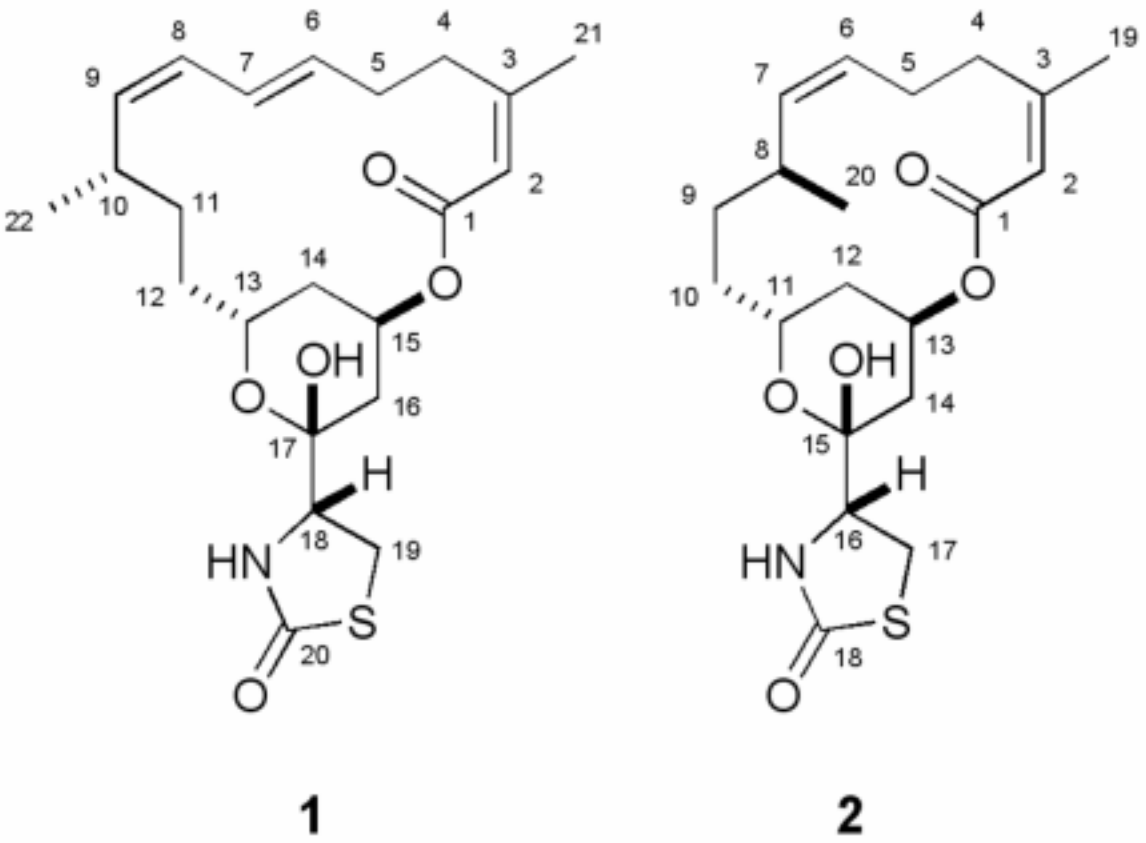

Somewhat surprising is that little side-by-side experimental therapeutic studies have been conducted on **1**, **2** and their analogs. In principle, these compounds are available from total syntheses[11–16] but such a pipeline has not been tapped. Few commercially available compound libraries have entities beyond **1** and **2**. Alternatively, it is possible to encounter these compounds in nature but the sources are restricted to the marine realm. This project was designed to further probe the biological activity properties of the latrunculin chemotype. Thus, the goals were to re-isolate **1** and **2**, obtain new analogs as a mini-library, and then evaluate them for their anti-actin and cancer cell line cytoxicity activities. Another goal was to use the isolation results to gain a better understanding of chemical ecology of both *N. magnifica* and *C. mycofijiensis* that are both reliable sources of these compounds. We believed this could be accomplished by examining selected collections housed in our repository.

Results and Discussion

Initially, the experimental design used in this study was influenced by insights obtained from evaluating literature to assess the breadth of latrunculin analogs isolated according to their

[a]Abbreviations: DFT, density functional theory; PKS/NRPS, polyketide synthase/non-ribosomal peptide synthetase; MAE, mean absolute error. Colon 38 (murine colon adenocarcinoma); L1210, murine lymphocytic leukemia; CFU-GM, murine bone marrow; HCT-116, human colorectal carcinoma; MDA-MB-435, human breast cancer; SRB, sulforhodamine B; A10, rat smooth muscle; DTP, developmental therapeutics program.

source organisms. Prior to our work outlined below, a total of 13 latrunculin family compounds had been reported, headed by **1**, **2** plus 11 analogs. Collectively, this information assembled in Table 1 (the entire list is shown in Table S1) indicated there was a diverse group of sponges as sources of these compounds. This data set contains the sponge taxonomic identification reported, the collection location, and the latrunculin frameworks observed among the isolated metabolites. There is no biological crossover between the occurrences of Red Sea sponges versus those from the Indo Pacific. Alternatively, with only one exception, **1** has been observed from all of the organisms listed. There are two main carbon frameworks present in these compounds, octa-ketide containing (Type 1), and hepta-ketide containing (Type 2). These can be further subdivided into the six distinct architectures based on the count of rings that are present: three (Types 1a or 2a), two (Types 1b, 2b or 2c), or one (Types 2d and 2e). There are two other significant structural features present among all the latrunculin family frameworks–all have *S* chirality at the carbon bearing the methyl group most distant from the ester carbonyl and the relative orientations of all three of the tetrahydropyran ring substituents are conserved. Other noteworthy chemical ecology patterns include: (a) the taxonomically unrelated sponges in Groups A and B, briefly noted above as *N. magnifica*[2] and *C. mycofijiensis*,[17] are a reliable source of latrunculin A, (b) we believe three sponges of Group C, *Dactylospongia*, *Fasciospongia*, and *Hyattella*, have been misidentified, and (c) one sponge of Group C was not identified. In summary, the significant chemical ecology insights based on Table 1 suggested that the most direct route to obtain a diverse mini-library of latrunculin frameworks would be through re-examination of *Negombata* specimens. Also, an extensive evaluation of *Cacospongia* collections was initially thought to be less useful due to their narrow chemical diversity as shown in Table 1.

The observations outlined above, dictated that the initial investigation begin on Red Sea-derived *N. magnifica*. Isolation work on a collection obtained in 2001 eventually afforded three known compounds, **2**,[1] 16-epi-latrunculin B (**3**)[8] and latrunculin C (**4**)[18] (Chart S1). An additional two compounds were added to this cache from our previous study of a 1988 collection of this species. These included the known 15-methoxylatrunculin B (**5**) and a one new analog at the point of publication, latrunculeic acid (**6**).[19] Overall these provided examples of the three of the six frameworks expected, including compounds of the Type 2a, 2b and 2e.

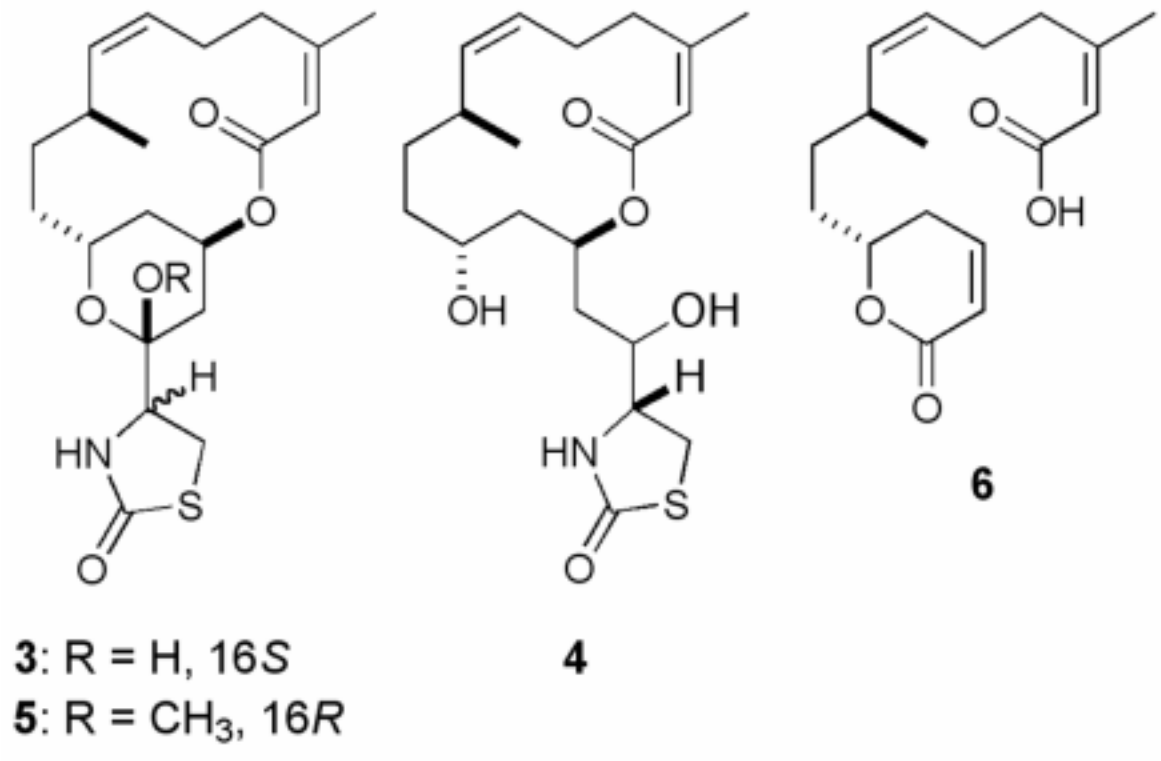

It appeared, based on the LCMS results (data not provided) of the crude extracts, that the only possibility for isolating additional chemotypes from *Cacospongia mycofijiensis* would occur through the investigation of minor components. This effort was begun with the large Fijian samplescollected in 1989 and 2000. Surprisingly, the 1989 collection (5.8 kg) was devoid **1**, but was a source for mycothiazole[20] and CTP-431[21] whose polyketide skeleton was closely related to that of **1**, plus minor amounts of new latrunculin derivatives that were not characterized. The isolation results for the 2000 collection [coll. # 00100-I and -II (1.9 kg and 0.6 kg)] were much more rewarding as eight compounds were obtained. The extraction method was the same as that described above and the resultant CH_2Cl_2 extract purified by reversed-phase HPLC (Chart S2) afforded: **1** and **2**, plus new analogs: latrunculol A (**7**), latrunculol B (**8**), 18-epi-latrunculol A (**9**), latrunculol C (**10**), latrunculone A (**11**), and latrunculone B (**12**). These compounds, which are Type 1a frameworks (Table 1), were valuable additions because they possessed highly modified macrocyclic rings. The known latrunculins isolated from the *Negombata* and *Cacospongia* sponges were identified by comparison of their ^{1}H and ^{13}C NMR data to those of published values. The data in support of structure shown for the six new entities follows next.

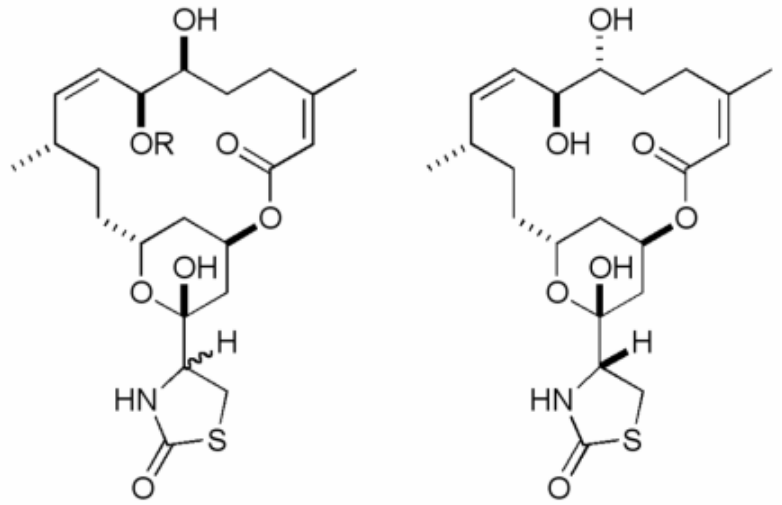

7: R = H, 18*R*
8: R = CH_3, 18*R*
9: R = H, 18*S*

10

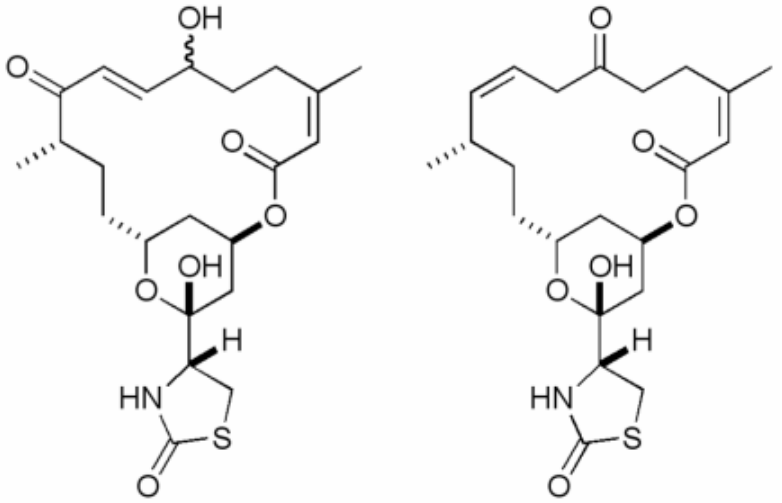

11 **12**

The elucidation of the planar structure for **7** was performed in a succinct manner once its molecular formula was established by HRESIMS as $C_{22}H_{33}NO_7S$. Relative to **1** there were two additional H and O atoms each and one less unsaturation equivalent. The diene chromophore of **1** was now present in **7** as a monoene diol, which was substantiated from the NMR data. The ^{1}H and ^{13}C NMR spectra of **7** revealed that vs. **1** signals of the Δ^{6} double bond of **1** were replaced by two oximethine signals (Tables 2 and 3) for a vicinal diol. Though the $^{3}J_{6,7}$ was not detectable, mutual gCOSY correlations were observed (Table S6). As expected, the remaining functional groups included: (1) a thiazolidinone carbonyl [δ 173.9 (C-20)], (2) an ester carbonyl [δ 166.6 (C-1)], (3) a disubstituted double bond [δ 5.64 (H-8), 5.05 (H-9), δ 132.3 (C-8), 136.5 (C-9)], (4) a trisubstituted double bond [δ 5.54 (H-2), δ 118.7

(C-2), 158.3 (C-3)] and (5) a hemiacetal quaternary carbon [δ 97.6 (C-17)]; all were consistent with the Type 1a system. Finally, the COSY and HMBC NMR data further substantiated (Table S6) the proposed planar structure of **7**.

Unraveling all the absolute stereochemical elements of **7** proved to be challenging. Establishing the spatial relationship between the three tetrahydropyran ring substituents plus that at C-18 was not the problem. These were readily determined from ^{1}H NMR coupling constant magnitudes. The large and small *J*s between H-13 and H-14a (*J* = 11.3 Hz), H-13 and H-14b (*J* = 3.8 Hz), and H-15 and H_2-16 ($J_{15,16a}$ = 4.3 and $J_{15,16b}$ = 2.0 Hz) mirrored that of **1**. Clearly, two of the groups appended to the chair conformation pyran ring, consisted of an equatorial C-13–C-12 bond, and an axial C-15–O, possessing 13*R**, 15*R** configurations. The C-17 and C-18 chirality was deduced to be 17*R** and 18*R** because of the parallel NMR data of **7** [δ 97.6 (C-17), δ 3.86, ddd, *J* = 8.6, 6.5 and 1.2 Hz (H-18), δ 63.4 (C-18)] versus **1**[δ 96.9 (C-17), δ 3.87, dd, *J* = 8 and 7 Hz (H-18), δ 62.1(C-18)][22] with *R* configuration at these sites. Next, the C-7 and C-10 centers were deduced to be 7*S** and 10*S** as a strong NOE correlation was observed between H-7 and H-10. The additional NOE correlation observed between H-10 and H-13 made it possible to further interrelate all three as 7*S**, 10*S**, and 13*R**. (Table S6). Tying in the relative stereochemistry at C-6 was accomplished through the NMR analysis of the acetonide **7a** obtained from **7** by treatment with 2,2-dimethoxypropane and pyridinium *p*-toluene sulfonate. The relatively large coupling constant of **7a** between H-6 and H-7 ($J_{6,7}$ = 8.6 Hz), and the NOEs observed from H-6 to H-8 and H-7 to H-10 as shown in Figure 1 all suggested a 6,7-anti configuration.[23] Therefore, the stereochemistry of H-6 was determined to be 6*S** building on the 7*S** assignment.

Converting the relative assignments enumerated above into absolute stereochemical designations was accomplished by examining the sensitivity of ^{13}C δs to changes in the C-6 and C-7 configurations. Such analysis for **7** was launched through DFT calculations, which involved comparing the experimental data to ^{13}C chemical shifts calculated for four possible diastereomers based on chirality changes at these two sites. The software Spartan 06 was employed and primed with the dual basis sets, B3LYP/6-31G*//B3LYP/6-31G* level.[24] We have previously demonstrated the power of the preceding basis sets as a calculation tool, and have defined the empirically derived expectation for acceptable agreement (experimental vs. calculated) assessed by an MAE < 2.2, and a % Score > 85.[25] The best agreement among the four diastereomers of **7** shown in Table 4 (and Tables S12–S15) was observed for the 6*S*, 7*S* isomer with % Score = 95 and the MAE = 2.1. Thus, the final assignments for **7** consist of 6*S*, 7*S*, 10*S*, 13*R*, 15*R*, 17*R*, 18*R*. These match those at the biosynthetically common chiral centers of **1** (at C-10, C-13, C-15, C-17 and C-18) whose absolute stereostructure has been unambiguously determined.[26]

The compounds **8**, **9** and **10** were close in structure to **7** and this simplified their characterizations. Compound **8** of $C_{23}H_{35}NO_7S$, had an extra CH_2 compared to that of **7** which was assigned as amethoxyl group (δ_H 3.24, s, δ_C 56.5). The 13C NMR signal (Tables 2 and 3) at C-7 in **8** was shifted upfield by 9 ppm vs. that of **7**, making the point of attachment for the OCH_3 group obvious, which was further confirmed by the 2D NMR data (Table S7). Parallel absolute chirality between **8** and **7** was proposed based on the nearly identical ^{1}H *J*s and ^{13}C δs at each chiral center. Compounds **9** ($C_{22}H_{33}NO_7S$) and **10** ($C_{22}H_{33}NO_7S$) were each diastereoisomers of **7** as each of the trio exhibited nearly similar ^{1}H and ^{13}C NMR properties (Tables S8 and S9). A minute, but distinct, difference between **9** and **7** was in the coupling constant patterns to H-18 (**9**: 3.92 td, *J* = 8.1 and 1.2 Hz, **7**: 3.86, ddd, *J* = 8.6, 6.5 and 1.2 Hz). Therefore, compound **9** was designated as 18-epi-latrunculol A. Additional support for this conclusion came by noting the ^{1}H NMR data at H-18 in **9** was parallel to that of the isostructural 16*S* proton of **3** (δ 3.87 ddd, *J* = 8.5, 8.5, and 1.0 Hz).[8] Thus, based on this consideration and analogy to **1**, the absolute chirality of **9** was deduced as 6*S*, 7*S*, 10*S*, 13*R*, 15*R*, 17*R*, 18*S*. The

last compound **10** was concluded to have identical relative configurations at C-17 and C-18 as compared to **1** and **7** due to congruence of the NMR data at these sites. In addition, NOEs (Table S9) between (a) H-10 and H-7, (b) H-13 and H-7, (c) H-13 and H-10, plus the diagnostic *J*'s to H-15 enabled assignment of the 7*S**, 10*S**, 13*R**, 15*R** configurations for **10**. Lastly, C-6 must be 6*R** to render **10** isomeric to **7**. To confirm this conclusion, the DFT calculated vs. experimental ^{13}C shifts obtained for the four C-6 and C-7 diastereormers of **10** were analyzed as shown in Table 4. The best fit was for 6*R*,7*S*, which gave a % Score = 95 and an MAE = 1.7 (Table 4 and Tables S16–S19). With this last assignment completed and by biogenetic analogy to the configurations in **1**, the absolute structure of latrunculol C was deduced to be 6*R*, 7*S*, 10*S*, 13*R*, 15*R*, 17*R*, 18*S*.

The last compounds to be characterized were **11** of $C_{22}H_{31}NO_7S$ and **12** of $C_{22}H_{31}NO_6S$, whose formulas were established from the HRESIMS data. The low field ^{13}C δs clarified that both possessed ketone residues. The allylic alcohol in **7** was replaced by a *trans*-enone in **11** recognized by signals at [δ 205.9 (C-9)] and [δ 7.03, dd, *J* = 16.3 and 8.6 Hz, (H-7), δ 5.96, d, *J* = 16.1 Hz (H-8), δ 149.6 (C-7), δ 132.0 (C-8)]. The planar structure of **11** (Table S9) was finalized by observing key HMBC correlations (H-22/C-9, H-8/C-10 and H-7/C-9) and key COSY correlations (H-6/H-7 and H-7/H-8). The geometry of the *trans* double bond at C-7–C-8 was also determined on the basis of 1D NOESY correlations from H-6 to H-8, from H-7 to H-10, and from H-13 to H-7. The NMR data of **12** indicated a homo conjugated *trans*-enone [δ 207.4 (C-6)] with a clearly visible bis-allylic methylene group [δ 2.96 and 3.35 (H_2-7), δ 41.5(C-7)]. The key COSY correlations (H-5/H-6 and H_2-7/H-8 and H-8/H-9) and HMBC correlations (H-5/C-6 and H-8/C-6) signified the planar structure **12**. The absolute configurations for **11** at the tetrahydropyrane and the thiazolidinone rings were deduced to be the same as those in **7**, **8** and **10** due to the similar proton and carbon NMR profiles at each of pertinent chiral centers. The 10*S* configuration was based on analogy to that of the latrunculin A congeners, but none of the data collected allowed definition of the stereochemistry at C-6. The absolute structure of **12** was provisionally assigned 10*S*, 13*R*, 15*R*, 17*R*, 18*R* based on its biogenetic relationship to **l**.

A mini-library of 13 compounds was obtained in sufficient quantity to engage in bioactivity assessment. This included 10 metabolites (**1**–**4**, **7**–**12**) isolated in this study, two latrunculin analogs (**5**, **6**) from our pure compound repository, and the synthetic derivative **7a**. Each was evaluated in the disk diffusion soft agar cell-based assay against murine cell lines shown in Figure 2: Colon 38, L1210 and CFU-GM.[27] Compounds were adsorbed onto the disk at a similar concentrations and a zone of inhibition (Z) in mm was recorded. Somewhat surprisingly, one of the new compounds, **7**, showed the best cytotoxic effect against Colon 38 (Z_{C38} = 23.5 mm at 1.1 μM), which was 2.6 and 1.8 times greater than **1** (Z_{C38} = 9.0 mm at 1.9 μM) and **2** (Z_{C38} = 13.0 mm at 5.1 μM), respectively. Four other compounds were almost as effective against Colon 38 and these included acetonide **7a** (Z_{C38} = 21.0 mm at 4.0 μM), **8** and **12** (each Z_{C38} = 19.5 mm at 1.1 μM), followed by **9** (Z_{C38} = 17.0 mm at 3.5 μM). Examining the relative sensitivity of the two other cell lines to these and the other compounds provided an assessment of their relative solid tumor selective cytotoxicity.[27] Four compounds fit this designation and are flagged by a * in Figure 2. These include **1**, **3**, **7** and **9** with Colon 38 selective in their cytotoxicity effect as follows. The magnitude of the differential selective cytotoxicity for **7** was identical to that of **1** (Z_{C38}–$Z_{CFU\text{-}GM}$ = 9.0 mm). Interestingly, compound **9** (Z_{C38}–$Z_{CFU\text{-}GM}$ = 15.0 mm), the 18*S* epimer of **7**, exhibited the greatest overall differential selective cytotoxicity. A similar enhancement of relative solid tumor selectivity was also seen when comparing the epimers, **3** (Z_{C38}–Z_{L1210} = 9.0 mm) and the 16*S* isomer, **2**, (Z_{C38}–Z_{L1210} = 1.5 mm). The next steps in this evaluation involved expanding the bioassay results by including additional cancer cell lines and this was done next.

Responses of two human solid cancer cell lines, HCT-116 and MDA-MB-435, were measured by trypane blue and SRB method, respectively, for all 13 compounds and the IC_{50} values are summarized in Table 5. Collectively this data showed significant inhibition for 7 of the 13 compounds and the trends against the HCT-116 cell line were somewhat similar to that observed in the disk diffusion assay. Overall, there were seven very active compounds led by **7** with the smallest IC_{50} = 0.48 μM against HCT-116. Other similarly active compounds (with HCT-116 IC_{50}'s in μM) included: **12** (0.92), **1** (1.1), **8** (2.1), **7a** (5.1), **9** (5.5), and **2** (7.1). The activity pattern against the MDA-MB-435 cell line was, with the exception of the response by **9** (IC_{50} > 50), almost parallel to that observed against HCT-116. The most active compound was **12** with an IC_{50} = 1.0 μM. The remaining order of activity was (with IC_{50}'s in μM): **7** (2.1), **1** (2.8), **2** (4.8), **8** (4.0), and **7a** (7.9). While these responses are appealing there is another important issue. Effective cytotoxins such as **1** and **2** that are powerful anti-actin agents are usually considered to be unsuitable for therapeutic development because of their unselective profile.[28] The IC_{50} ratios tabulated in the 3rd column of Table 5 for the latter six compounds could be interpreted as consistent with this view. Alternatively, the very different ratio computed for **9** could foreshadow a special circumstance. This possibility was investigated next.

The mini-library was further assessed in a microfilament-disrupting assay using A10 cells.[29] Figure 3 shows the results of the phenotypic assay used and the last column of Table 5 summarizes the level of anti-actin action at 5 μM for each of the compounds. Our results are consistent with previous studies that show, relative to the control, the expected microfilament-modulating effects were exhibited by **1** and **2**. We also observed, as shown in Figure 3, significant disruption action by **3** and **7**. Analogous perturbation effects were observed (not shown here but tabulated in Table 5) for **7a**, **8**, **10**, **12** at 5 μM. By contrast, the response for **9** while not identical to the control (Figure 3), represents the pattern expected for a compound devoid of significant microfilament-disrupting action. Similar negative responses were observed for four other compounds, **4**, **5**, **6**, and **11**. Overall, these results when evaluated side-by-side with the cytotoxicity data indicate that six of the seven very active compounds (**1**, **2**, **7**, **7a**, **8**, **12**) are aggressive actin disruptors. The different profile for **9** is intriguing and apparently a variation in the 18*R* to 18*S* configuration of the thiazolidinone ring (**7** vs. **9**) diminishes the anti-actin effect without eliminating the cytototxicity properties. This pattern does not appear to hold for the latrunculin B series as the microfilament-disrupting activities were similar for **2** vs. **3**, in which the configuration at 16 changes from *R* to *S*.

It is worthwhile to further discuss one additional activity trend has emerged from this study. More than 50% of the latrunuculin analogs (7 compounds) evaluated in this cell based assay study were significantly active (IC_{50}'s = 0.5–10 μM) against one or both cell lines. All of these compounds possess the Type 1a framework. The remaining 6 compounds had modest to inactive IC_{50}'s, and this group included all 4 of the Type 2 framework compounds plus 2 with a Type 1a framework. The conformation of the 16-membered macrolide ring appears to be critical for activity as judged by the significant activity of **1**, **7**, **7a**, **8** and **12**, vs. the poor responses for **10** and **11**. Not to be ignored is the requirement for the *R* configuration of the thiazolidinone ring for maximizing IC_{50} against human tumor cell lines.

Conclusions

Our findings have increased the understanding about the latrunculin family chemotypes and their cytotoxicity properties. We obtained both **1** and **2** from a Fijian *C. mycofijiensis*, which represents the first example of Type 1 and 2 structures co-occurring in *Cacospongia*. The isolation and characterization of **7**–**11** possessing unprecedented new macrolide oxygenation patterns serves to further extend the record of structural information. The discovery that there are two distinct cytotoxicity modes of action operating for the latrunculin family, illustrated

by the data in Table 5 for **1**, **7**, **12** vs. **9**, should stimulate further interest in experimental therapeutics investigations of these compounds. The NCI database contains information about **1** (NSC 613011) and **2** (NSC 339663), but these records have been generally ignored or are unavailable to the scientific community. As another important forgotten finding, Longley demonstrated that **1** was remarkably activity against A549 lung tumor xenograft mouse model (T/C = 146%).[30] This provides an important counter point to the observations of the DTP/NCI group that have not been able to "demonstrate a realistic therapeutic index"[28] for any cytotoxic actin inhibitor. At this juncture we have initiated efforts to further probe the preclinical potential of three new leads, **7**, **9** and **12**. The properties of **9** are especially important as they are similar to those of oxolatrunculin B,[31] as each may inhibit cancer cell line growth by an actin independent pathway.

Experimental Section

General Experimental Procedures

Optical rotations were obtained on a digital polarimeter. The NMR spectra were recorded in $CDCl_3$ and acetone-d_6 at 500 and 600 MHz for 1H and 125.6 and 150.0 MHz for ^{13}C, respectively. Semi preparative HPLC was performed using a 5 μm C_{18} ODS column by means of a single wavelength (λ = 230 nm) for compound detection. High resolution mass measurements were obtained from an ESI-TOF mass spectrometer. DFT calculations were performed by Spartan 06 with a basis set B3LYP/6-31G*//B3LYP/6-31G* level. The computer used for DFT calculations was equipped with a dual 2.80 GHz CPU and 4 GB DDR2 SDRAM at 667 MHz with 222 GB disk space.

Biological Material, Collection, and Identification

Specimens of *N. magnifica*[19] (coll. no. 01600) (0.62 kg wet weight) were collected using SCUBA in 2001 off the coast of Eilat, Israel at depths of 15m. Two separate specimens of *C. mycofijiensis*[32] (coll. no. 00100 I and II) (1.9 & 0.6 kg wet weight) were collected using SCUBA in 2000 from the Beqa Lagoon, Fiji, at depths of 15–20 m. Taxonomic identification was based on comparison of the biological features to other samples in our repository and physical features of those previously published.[19,32] Voucher specimens and underwater photos are available.

DFT calculations for carbon chemical shifts

The carbon chemical shifts predicted by Spartan 06 were corrected by least-square method.[33] Score was defined by an equation [# of carbon–points/# of carbon x 100 (%)]. The points (0–3 points) are given on the basis of the absolute difference between predicted carbon and experimental carbon chemical shift: (1) 0 points (< 5 ppm), (2) 1 point (6–10 ppm), (3) 2 points (11–20 ppm), and (4) 3 points (> 21 ppm).

Biological Assays

The detailed methods of the disk diffusion soft agar colony formation assay, IC_{50} determination for HCT-116 and MDA-MB-435, microfilament-disrupting assay, are described previously.[34] The assay results appear in Figures 2 and 3 and Table 5.

Extraction and Isolation

Samples were preserved in the field according to our standard laboratory procedures and stored in a cold room until extraction was performed. The sponges were extracted 3× with methanol and then the resultant oil was partitioned using a modified Kupchan-type solvent partition scheme.[35] The CH_2Cl_2 extract (FD, 180 mg) of the sponge, *N. magnifica*, (coll. # 01600) was fractionated using repeated semi-preparative reverse phase gradient HPLC (80:20 CH_3CN/H_2O up to 100% over 40 minutes) to give six fractions. Fraction H3 (7.8 mg) was then further

purified using the above conditions to yield **4** (3.3mg). Fractions H4 (51.2 mg) and H5 (11.3 mg) afforded **2** and **3**. The CH_2Cl_2 extract (FD, 75 mg) of the sponge, *C. mycofijiensis*, (coll. # 00100-I) was also purified using repeated semi preparative reversed-phase gradient HPLC (30:70 CH_3CN/H_2O up to 80:20 over 50 minutes) to give nine fractions. The resultant fractions H1-H9 eluted in the following order and afforded **10** (1.6 mg), **7** (8.3 mg), **9** (2.5 mg), **11** (2.6 mg), **8** (3.1 mg), **12** (2.8 mg), **1** (25.3 mg). Fractions H5 and H9 were not fully pursued due to limited sample size and purity. A separate purification of the lesser CH_2Cl_2 extract (00100-II FD, 75 mg) was made using the same HPLC conditions and generated eleven fractions. Additional amounts of compounds **1** and **7**–**12** were obtained along with **2** (2.2 mg).[22] These isolation procedures for the sponges, *N. magnifica* (coll # 01600) and *C. mycofijiensis* (coll # 00100) were described in Chart S1 and S2 respectively.

Latrunculin A (1): white powder; $[\alpha]^{23}_D$ +144.4 (*c* 1.0, $CHCl_3$); 1H and 13C NMR data see Table S1; HRESITOFMS *m/z* 444.1827 $[M+Na]^+$ (calcd for $C_{22}H_{31}NO_5SNa$ 444.1815). This compound was identified by comparison of spectral data with those of the literature values.[22]

Latrunculin B (2): white powder; $[\alpha]^{23}_D$ +120.1 (*c* 4.0, $CHCl_3$); 1H and 13C NMR data see Table S2; HRESITOFMS *m/z* 418.1653 $[M+Na]^+$ (calcd for $C_{20}H_{29}NO_5SNa$ 418.1659). This compound was identified by comparison of spectral data with those of the literature values.[22]

16-epi-Latrunculin B (3): white powder; $[\alpha]^{23}_D$ + 81.2 (*c* 1.0, $CHCl_3$); 1H and 13C NMR data see Table S3; HRESITOFMS *m/z* 418.1649 $[M+Na]^+$ (calcd for $C_{20}H_{29}NO_5SNa$ 418.1659). This compound was identified by comparison of spectral data with those of the literature values.[8]

Latrunculin C (4): white powder; ^1H and ^{13}C NMR see Table S4; HRESITOFMS *m/z* 420.1815 $[M+Na]^+$ (calcd for $C_{20}H_{31}NO_5SNa$ 420.1798). This compound was identified by comparison of spectral data with those of the literature values.[18]

Library compounds: 15-methoxylatrunculin B (**5**) and latrunculeic acid (**6**) were used for the disk diffusion cell-based assay. The purity (> 95%) for **5** and **6** was confirmed by LCMS and ^1H NMR analysis.[19,36]

Latrunculol A (7): white powder; $[\alpha]^{26}_D$ +64.8 (*c* 5.6, MeOH); UV (MeOH) λ_{max} (log ε) 216 nm (4.07); ^1H and ^{13}C NMR data see Tables 2, 3 and S5; HRESITOFMS *m/z* 478.1864 $[M+Na]^+$ (calcd for $C_{22}H_{33}NO_7SNa$ 478.1870).

Formation of acetonide 7a from 7

To a solution of 7 (5.0 mg) in CH_2Cl_2 (0.5 mL) were added 2,2-dimethoxypropane (0.75 mL) and pyridinium toluene-*p*-sulfonate (9.0 mg). After stirring of the mixture at room temperature for 2 h, the solvent was evaporated off under reduced pressure. The residue was purified by HPLC using acetonitrile–water (1:1 to 1:0) as the eluent to afford acetonide 7a (2.5 mg) as a colorless powder.

Acetonide 7a: colorless powder; $[\alpha]^{28}_D$ +21.7 (*c* 1.7, MeOH); 1H NMR δ ppm ($CDCl_3$) 5.70 (1H, d, *J* = 1.4 Hz, H-2), 5.64 (1H, br. s, NH), 5.44 (1H, dd, *J* = 10.7 and 9.6 Hz, H-9), 5.39 (1H, dd, *J* = 10.8 and 8.7 Hz, H-8), 5.38 (1H, m, H-15), 4.45 (1H, t, *J* = 8.5 Hz, H-7), 4.05 (1H, br. t, 9.8 Hz, H-13), 3.83 (1H, ddd, *J* = 8.8, 5.6 and 1.0 Hz, H-18), 3.77 (1H, ddd, *J* = 8.6, 5.9 and 4.3 Hz, H-6), 3.50 (1H, dd, *J* = 11.6, 8.9 Hz, H-19b), 3.41 (1H, dd, *J* = 11.6 and 6.0 Hz, H-19a), 2.55–2.63 (3H, m, H_2-4 and H-10), 2.08 (1H, dt, *J* = 14.6 and 2.2 Hz, H-16b), 1.95 (3H, s, H_3-21), 1.90 (1H, br.d, *J* = 14.6 Hz, H-16a), 1.67–1.76 (5H, m, H_2-5, H-11b and H-14b), 1.40–1.56 (3H, m, H_2-12, H-14a), 1.44 (3H, s, H_3-acetonide), 1.43 (3H, s, H_3-acetonide), 1.20 (1H, m, H-11a), 1.02 (3H, d, *J* = 5.5 Hz, H_3-22); NOESY1D (mixing time =

0.5 ms) H-8/H-6, H-7/H-10; HRESIMS *m/z* 518.2178 $[M+Na]^+$ (calcd for 518.2183, $C_{25}H_{37}NO_7SNa$).

Latrunculol B (8): white powder; $[\alpha]^{27}_D$ +47.5 (*c* 1.6, MeOH); UV (MeOH) λ_{max} (log ε) 216 nm (3.95); ^1H and ^{13}C NMR data see Tables 2, 3 and S7. HRESITOFMS *m/z* 492.2025 $[M+Na]^+$; (calcd for $C_{23}H_{35}NO_7SNa$ 492.2027).

18-epi-Latrunculol A (9): white powder; $[\alpha]^{27}_D$ +55.2 (*c* 4.4, MeOH); UV (MeOH) λ_{max} (log ε) 216 nm (4.06); ^1H and ^{13}C NMR data in Figures S15, S16 and Table S8; HRESITOFMS *m/z* 478.1866 $[M+Na]^+$; (calcd for $C_{22}H_{33}NO_7SNa$ 478.1870).

Latrunculol C (10): white powder; $[\alpha]^{28}_D$ +56.1 (*c* 1.3, MeOH); UV (MeOH) λ_{max} (log ε) 216 nm (4.50); ^1H and ^{13}C NMR data see Tables 2, 3 and S9; HRESITOFMS *m/z* 478.1878 $[M+Na]^+$; (calcd for $C_{22}H_{33}NO_7SNa$ 478.1870).

Latrunculone A (11): white powder; $[\alpha]^{27}_D$ +5.8 (*c* 1.2, MeOH); UV (MeOH) λ_{max} (log ε) 216 nm (4.23); ^1H and ^{13}C NMR data see Tables 2, 3 and S10; HRESITOFMS *m/z* 476.1707 $[M+Na]^+$ (calcd for $C_{22}H_{31}NO_7SNa$ 476.1714).

Latrunculone B (12): white powder; $[\alpha]^{29}_D$ +129.2 (*c* 0.1, MeOH); 1H and 13C NMR data see Tables 2, 3 and S11; HRESITOFMS *m/z* 460.1764 $[M+Na]^+$; (calcd for $C_{22}H_{31}NO_6SNa$ 460.1735).

Supplementary Material

Refer to Web version on PubMed Central for supplementary material.

Acknowledgments

This work was supported by the National Institute of Health R01 CA 47135, NMR equipment grants NSFCHE-0342912 and NIH S10-RR19918, MS equipment grant NIH S10-RR20939 and funding from the Joe and Jessie Crump Foundation (SLM). We thank C. P Loo and D. B. Cordes for the initial isolation work of *C. mycofijiensis*. We also thank D. LaBoeuf for her excellent technical assistant. We thank M. Ilan and the members of the Ilan Research Group for their generous assistance in the permit acquisition and collection of *N. magnifica.* We are also grateful to W. Aalbersberg, University of the South Pacific, Fiji and A. Raiwalui, Permanent Secretary for the Director of Fisheries, Ministry of Agriculture, Fisheries and Forests Division, for obtaining administrative approvals to carry out research in Fiji.

References and Notes

1. Kashman Y, Groweiss A, Shmueli U. Latrunculin, a New 2-Thiazolidinone Macrolide from the Marine Sponge *Latrunculia magnifica*. Tetrahedron Lett 1980;21:3629–3632.
2. Spector I, Shochet NR, Kashman Y, Groweiss A. Latrunculins: Novel Marine Toxins That Disrupt Microfilament Organization in Cultured Cells. Science 1983;219:493–495. [PubMed: 6681676]
3. Sonnenschein RN, Johnson TA, Tenney K, Valeriote FA, Crews P. A Reassignment of (−)-Mycothiazole and the Isolation of a Related Diol. J Nat Prod 2006;69:145–147. [PubMed: 16441088]
4. Gerth K, Bedorf N, Hoefle G, Irschik H, Reichenbach H. Antibiotics from Gliding Bacteria. 74. Epothilons A and B: Antifungal and Cytotoxic Compounds from *Sorangium cellulosum* (Myxobacteria): Production, Physico-Chemical and Biological Properties. J Antibiot 1996;49:560–563. [PubMed: 8698639]
5. Hoefle G, Bedorf N, Steinmetz H, Schomburg D, Gerth K, Reichenbach H. Antibiotics from Gliding Bacteria. 77. Epothilone A and B - Novel 16-Membered Macrolides with Cytotoxic Activity: Isolation, Crystal Structure, and Conformation in Solution. Angew Chem, Int Ed Engl 1996;35:1567–1569.
6. Coue M, Brenner SL, Spector I, Korn ED. Inhibition of Actin Polymerization by Latrunculin A. FEBS Lett 1987;213:316–318. [PubMed: 3556584]

7. Hayot C, Debeir O, Van Ham P, Van Damme M, Kiss R, Decaestecker C. Characterization of the Activities of Actin-Affecting Drugs on Tumor Cell Migration. Toxicol Appl Pharmacol 2006;211:30–40. [PubMed: 16005926]
8. Hoye TR, Ayyad SEN, Eklov BM, Hashish NE, Shier WT, El Sayed KA, Hamann MT. Toward Computing Relative Configurations: 16-epi-Latrunculin B, a New Stereoisomer of the Actin Polymerization Inhibitor Latrunculin B. J Am Chem Soc 2002;124:7405–7410. [PubMed: 12071749]
9. Ayscough KR, Stryker J, Pokala N, Sanders M, Crews P, Drubin DG. High Rates of Actin Filament Turnover in Budding Yeast and Roles for Actin in Establishment and Maintenance of Cell Polarity Revealed Using the Actin Inhibitor Latrunculin-A. J Cell Biol 1997;137:399–416. [PubMed: 9128251]
10. Morton WM, Ayscough KR, McLaughlin PJ. Latrunculin Alters the Actin-Monomer Subunit Interface to Prevent Polymerization. Nat Cell Biol 2000;2:376–378. [PubMed: 10854330]
11. Furstner A, De Souza D, Parra-Rapado L, Jensen JT. Catalysis-Based Total Synthesis of Latrunculin B. Angew Chem, Int Ed Engl 2003;42:5358–5360. [PubMed: 14613176]
12. White JD, Kawasaki M. Total Synthesis of (+)-Latrunculin A, an Ichthyotoxic Metabolite of the Sponge *Latrunculia magnifica* and Its C-15 Epimer. J Org Chem 1992;57:5292–5300.
13. White JD, Kawasaki M. Total Synthesis of (+)-Latrunculin A. J Am Chem Soc 1990;112:4991–4993.
14. Smith AB III, Noda I, Remiszewski SW, Liverton NJ, Zibuck R. Total Synthesis of (+)-Latrunculin A. J Org Chem 1990;55:3977–3979.
15. Zibuck R, Liverton NJ, Smith AB III. Total Synthesis of (+)-Latrunculin B. J Am Chem Soc 1986;108:2451–2453.
16. Fuerstner A, De Souza D, Turet L, Fenster MDB, Parra-Rapado L, Wirtz C, Myott R, Lehmann CW. Total Syntheses of the Actin-Binding Macrolides Latrunculin A, B, C, M, S and 16-epi-Latrunculin B. Chem--Eur J 2006;13:115–134.
17. Kakou Y, Crews P, Bakus GJ. Dendrolasin and Latrunculin A from the Fijian Sponge *Spongia mycofijiensis* and an Associated Nudibranch *Chromodoris lochi*. J Nat Prod 1987;50:482–484.
18. Kashman Y, Groweiss A, Lidor R, Blasberger D, Carmely S. Latrunculins: NMR Study, Two New Toxins and a Synthetic Approach. Tetrahedron 1985;41:1905–1914.
19. Vilozny B, Amagata T, Mooberry SL, Crews P. A New Dimension to the Biosynthetic Products Isolated from the Sponge *Negombata magnifica*. J Nat Prod 2004;67:1055–1057. [PubMed: 15217296]
20. Crews P, Kakou Y, Quinoa E. Mycothiazole, a Polyketide Heterocycle from a Marine Sponge. J Am Chem Soc 1988;110:4365–4368.
21. Johnson TA, Amagata T, Oliver AG, White KN, Tenney K, Valeriote FA, Crews P. The unexpected isolation of CTP-431, a novel thiopyrone from the sponge Cacospongia mycofijiensis. J Org Chem. In press
22. Groweiss A, Shmueli U, Kashman Y. Marine Toxins of *Latrunculia magnifica*. J Org Chem 1983;48:3512–3516.
23. Nagle DG, Gerwick WH. Structure and Stereochemistry of Constanolactones A-G, Lactonized Cyclopropyl Oxylipins from the Red Marine Alga *Constantinea simplex*. J Org Chem 1994;59:7227–7237.
24. Spartan 06. Wavefunction, Inc; Irvine, CA: http://www.wavefun.com
25. Amagata T, White KN, Wenzel PJ, Crews P. unpublished results
26. Jefford CW, Bernardinelli G, Tanaka J, Higa T. Structures and Absolute Configurations of the Marine Toxins, Latrunculin A and Laulimalide. Tetrahedron Lett 1996;37:159–162.
27. Valeriote F, Grieshaber Charles K, Media J, Pietraszkewicz H, Hoffmann J, Pan M, McLaughlin S. Discovery and Development of Anticancer Agents from Plants. J Exp Ther Oncol 2002;2:228–236. [PubMed: 12416027]
28. Newman DJ, Cragg GM. Marine Natural Products and Related Compounds in Clinical and Advanced Preclinical Trials. J Nat Prod 2004;67:1216–1238. [PubMed: 15332835]
29. Mooberry SL, Tien G, Hernandez AH, Plubrukarn A, Davidson BS. Laulimalide and Isolaulimalide, New Paclitaxel-Like Microtubule-Stabilizing Agents. Cancer Res 1999;59:653–660. [PubMed: 9973214]

30. Longley RE, McConnell OJ, Essich E, Harmody D. Evaluation of Marine Sponge Metabolites for Cytotoxicity and Signal Transduction Activity. J Nat Prod 1993;56:915–920. [PubMed: 8350092]

31. Ahmed SA, Odde S, Daga PR, Bowling JJ, Mesbah MK, Youssef DT, Khalifa SI, Doerksen RJ, Hamann MT. Latrunculin with a Highly Oxidized Thiazolidinone Ring: Structure Assignment and Actin Docking. Org Lett 2007;9:4773–4776. [PubMed: 17929935]

32. Sanders, ML.; van Soest, RWM. A Revised Classification of *Spongia mycofijiensis*. In Recent Advances in Sponge Biodiversity Inventory and Documentation. In: Willenz, P., editor. Bull Inst R Sci Nat Bel Biol. Vol. 66. 1996. p. 117-122.

33. Rychnovsky SD. Predicting NMR Spectra by Computational Methods: Structure Revision of Hexacyclinol. Org Lett 2006;8:2895–2898. [PubMed: 16774284]

34. Johnson TA, Tenney K, Cichewicz RH, Morinaka BI, White KN, Amagata T, Subramanian B, Media J, Mooberry SL, Valeriote FA, Crews P. Sponge-Derived Fijianolide Polyketide Class: Further Evaluation of Their Structural and Cytotoxicity Properties. J Med Chem 2007;50:3795–3803. [PubMed: 17622130]

35. Thale Z, Johnson T, Tenney K, Wenzel PJ, Lobkovsky E, Clardy J, Media J, Pietraszkiewicz H, Valeriote FA, Crews P. Structures and Cytotoxic Properties of Sponge-Derived Bisannulated Acridines. J Org Chem 2002;67:9384–9391. [PubMed: 12492342]

36. Blasberger D, Carmely S, Cojocaru M, Spector I, Shochet NR, Kashman Y. On the Chemistry of Latrunculins A and B. Liebigs Ann Chem 1989:1171–1188.

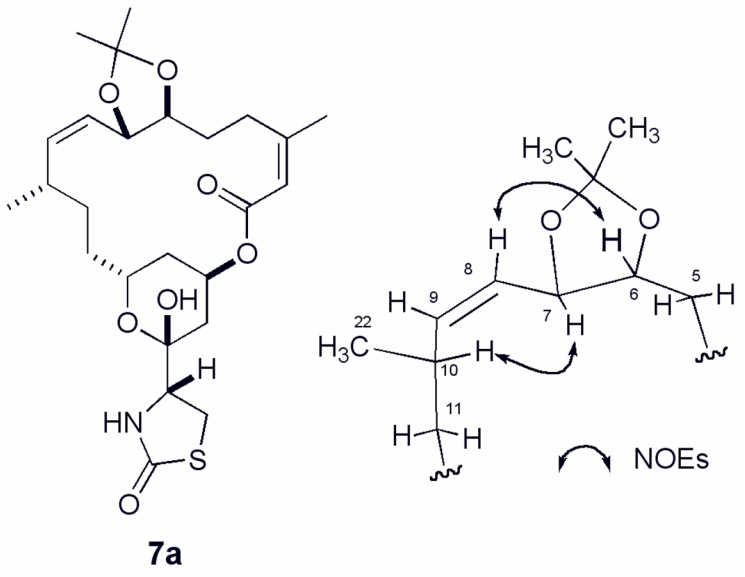

Figure 1.
Structure of acetonide **7a** and its key NOEs.

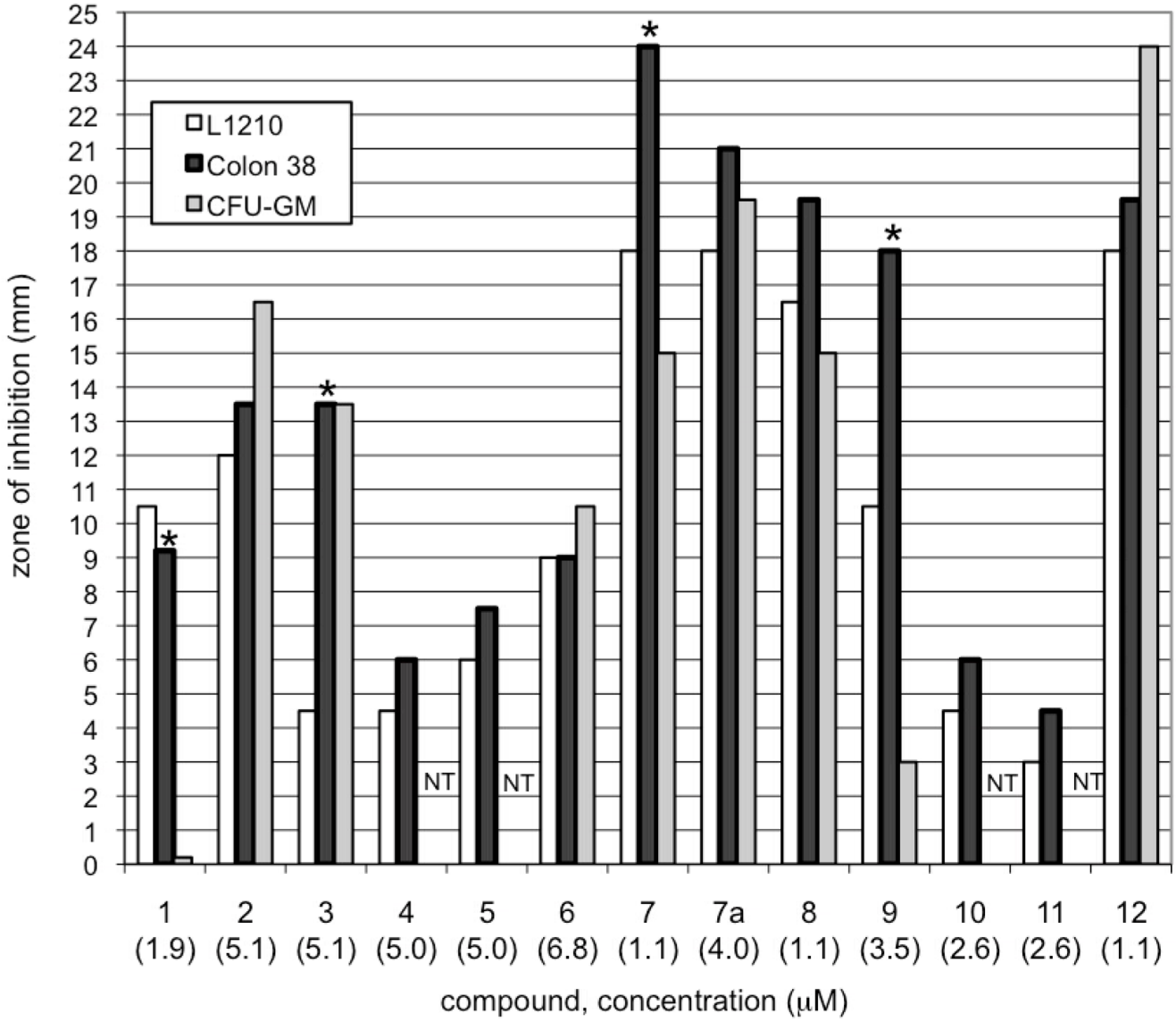

Figure 2.

Cytotoxicity against murine cell lines for **1**–**12** and **7a**. * Selective cytotoxicity (> 7.5 mm difference) for murine cell lines, L1210, Colon 38, CFU-GM. Each compound was applied onto a disk with 15 μL of DMSO solution of the concentration given in the figure. NT = not tested. DMSO used as a control showed no ctotoxicity against all the cell lines (zone inhibition = 0 mm).

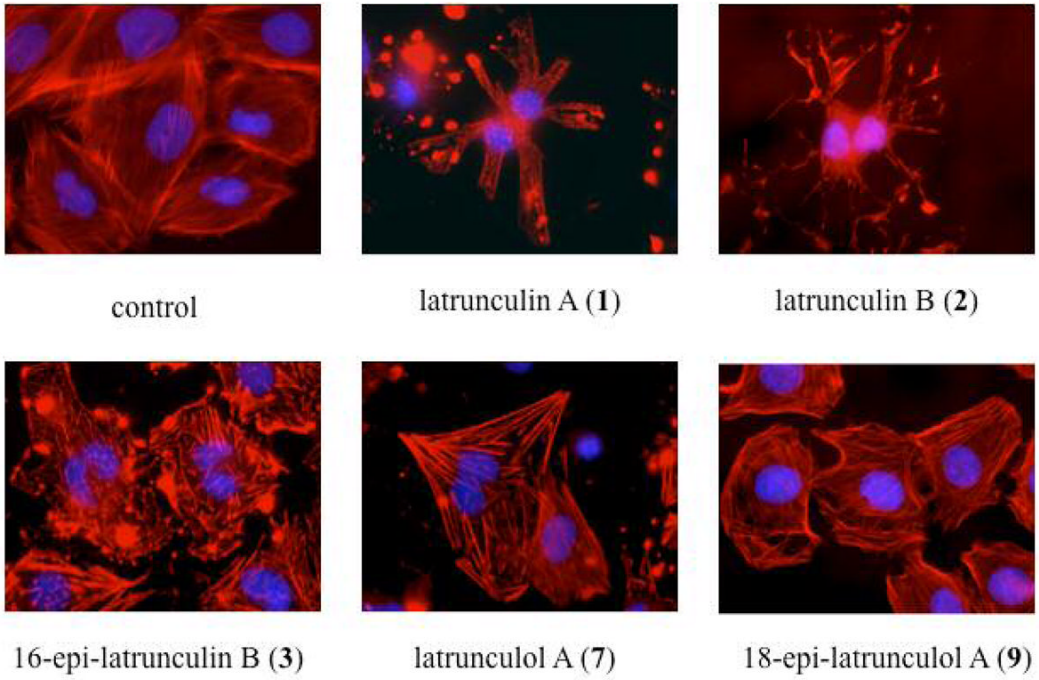

Figure 3.
Microfilament disrupting effect of compounds **1**, **2**, **3**, **7** and **9** at 5μM against A10 cells

Table 1

Summary of Latrunculin Frameworks and Their Biological Sources[a]

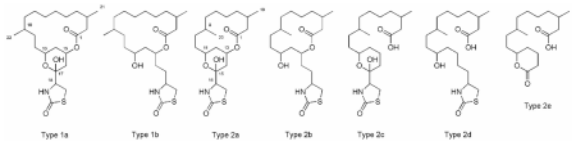

	taxnomic identification	collection site	Type 1		Type 2				
			1a	1b	2a	2b	2c	2d	2e
Group A	*Negombata magnifica*	Dahlak Archipelago	x						
		Djibouti	x		x				
		Egypt	x		x			x	
		Israel			x	x			x
		Tiran Straits	x		x			x	
		not specified	x				x		
	N. corticata	Egypt			x				
Group B	*Cacospongia mycofijiensis*	Fiji	x						
		Indonesia	x						
		Marshall Islands	x						
		Papua New Guinea	x						
		Solomon Islands	x						
		Tonga	x						
		Vanuatu	x						
Group C	*Dactylospongia* sp.	Vanuatu	x						
	Fasciospongia rimosa	Okinawa	x	x					
	Hyattella sp.	Indonesia	x						
	unidentifiable	American Samoa	x						

[a]The entire list including cited literature is shown in Table S1

Table 2

^{1}H NMR Data for **7**–**12** (600 MHz)

position	**7**[a] δ_H (mult, *J* in Hz)	**8**[a] δ_H (mult, *J* in Hz)	**9**[a] δ_H (mult, *J* in Hz)	**10**[a] δ_H (mult, *J* in Hz)	**11**[a] δ_H (mult, *J* in Hz)	**12**[b] δ_H (mult, *J* in Hz)
2	5.54 (q, 1.0)	5.55 (q, 1.0)	5.56 (q, 1.2)	5.63 (q, 1.0)	5.59 (q, 1.2)	5.69 (q, 1.2)
4a	2.58 (td, 11.6, 5.4)	2.54 (td, 11.4, 5.4)	2.57 (td, 11.5, 5.3)	2.59 (ddd, 13.4, 10.4, 6.3)	2.35 (td, 12.0, 5.3)	2.26 (ddd, 13.2, 8.4, 6.0)
4b	2.63 (td, 11.6, 5.2)	2.66 (td, 11.4, 5.2)	2.69 (td, 11.5, 5.0)	3.34 (ddd, 13.4, 10.3, 5.2)	2.96 (td, 12.0, 6.2)	3.29 (ddd, 13.2, 9.0, 7.2)
5a	1.82 (m)	1.81 (m)	1.81 (m)	1.84 (m)	1.84 (2H, m)	2.61 (ddd, 15.6, 9.0, 7.2)
5b	1.88 (m)	1.86 (m)	1.88 (m)	1.94 (m)		2.73 (ddd, 14.4, 8.4, 6.0)
6	3.36 (dd, 8.9, 4.5, 1.5)	3.34 (br. s)	3.38 (ddd, 9.1, 4.5, 1.5)	3.53 (ddd, 8.2, 5.0, 3.1)	4.31 (td, 8.4, 4.1)	
7a	4.34 (d, 9.6)	3.99 (d, 9.8)	4.37 (d, 9.6)	4.26 (t, 8.4)	7.03 (dd, 16.3, 8.6)	2.96 (ddd, 17.4, 6.6, 1.8)
7b						3.35 (ddd, 17.2, 6.2, 1.1)
8	5.64 (t, 10.3)	5.57 (t, 10.3)	5.65 (t, 10.3)	5.35 (dd, 11.0, 8.6)	5.96 (d, 16.1)	5.45 (dddd, 10.8, 9.6, 6.6, 0.6)
9	5.05 (td, 10.9, 1.0)	5.33 (td, 10.9, 1.0)	5.07 (td, 10.9, 1.0)	5.21 (t, 11.0)		5.33 (m)
10	2.73 (m)	2.81 (m)	2.78 (m)	2.68 (m)	3.69 (m)	2.40 (m)
11a	1.06 (ddt, 13.7, 11.5, 4.0)	1.10 (ddt, 13.7, 11.4, 3.8)	1.07 (ddt, 13.6, 11.5, 4.0)	1.13 (m)	1.60 (dddd, 13.2, 11.5, 4.8, 3.1)	1.16 (dddd, 13.6, 9.5, 5.7, 3.3)
11b	1.89 (m)	1.93 (m)	1.96 (m)	1.55 (m)	1.82 (m)	1.66 (m)
12a	1.45 (2H, m)	1.47 (2H, m)	1.47 (2H, m)	1.54 (2H, m)	1.29 (dddd, 14.2, 12.5, 4.8, 3.4)	1.48 (2H, m)
12b					1.42 (dddd, 14.2, 11.5, 4.3, 3.0)	
13	4.29 (tdd, 11.3, 3.8, 1.9)	4.29 (tdd, 11.3, 3.8, 1.9)	4.33 (tdd, 11.3, 3.6, 2.1)	4.57 (m)	4.35 (dt, 11.6, 2.8)	3.88 (tdd, 10.2, 4.2, 2.4)
14a	1.59 (ddd, 14.7, 11.3, 3.8)	1.60 (ddd, 14.8, 11.3, 3.8)	1.61 (ddd, 14.8, 11.3, 3.6)	1.52 (ddd, 14.4, 7.8, 2.9)	1.53 (ddd, 14.6, 11.6, 3.4)	1.42 (ddd, 15.0, 12.0, 3.0)
14b	1.80 (m)	1.83 (m)	1.82 (m)	2.04 (m)	1.65 (ddd, 14.4, 4.8, 2.1)	2.02 (m)
15	5.19 (m)	5.21 (m)	5.16 (m)	5.29 (m)	5.30 (m)	5.33 (m)
16a	1.81 (dd, 14.9, 4.3)	1.84 (dd, 14.9, 4.3)	1.79 (dd, 14.9, 4.2)	1.88 (dd, 14.6, 4.1)	1.86 (dd, 15.1, 4.3)	1.92 (dt, 14.4, 3.6)
16b	2.25 (dt, 14.9, 2.0)	2.26 (dt, 14.9, 2.0)	2.17 (dt, 14.9, 2.0)	2.14 (dt, 14.6, 2.1)	2.15 (dt, 15.1, 2.2)	2.08 (dt, 14.4, 1.8)
18	3.86 (ddd, 8.6, 6.5, 1.2)	3.86 (ddd, 8.6, 6.5, 1.2)	3.92 (td, 8.1, 1.2)	3.87 (ddd, 8.9, 6.5, 1.2)	3.91 (ddd, 8.8, 6.5, 1.2)	3.82 (ddd, 9.0, 6.0, 1.2)
19a	3.45 (dd, 11.5, 8.6)	3.45 (dd, 11.5, 8.6)	3.43 (dd, 11.2, 7.7)	3.44 (dd, 11.5, 8.9)	3.47 (dd, 11.5, 8.7)	3.41 (dd, 11.4, 6.0)
19b	3.48 (dd, 11.5, 6.5)	3.48 (dd, 11.5, 6.5)	3.45 (dd, 11.2, 8.1)	3.48 (dd, 11.5, 6.3)	3.51 (dd, 11.5, 6.3)	3.48 (dd, 11.4, 9.0)
21	1.90 (d, 1.5)	1.92 (d, 1.5)	1.92 (d, 1.5)	1.92 (d, 1.2)	1.92 (d, 1.5)	1.90 (d, 1.2)
22	0.92 (d, 6.5)	0.97 (d, 6.5)	0.94 (d, 6.7)	0.94 (d, 6.4)	0.99 (d, 6.9)	0.94 (d, 6.6)
NH	7.04 (br. s)	7.05 (br. s)	6.58 (br. s)	6.97 (br. s)	7.13 (br.s)	5.71 (br. s)
6-OH	4.83 (br. s)	3.12 (br. s)	nd	3.22[d] (br. s)	5.12[e] (br. s)	
7-OH	3.59[c] (br. s)		nd	3.75[d] (br. s)		
17-OH	nd[c]	4.84 (br. s)	nd	4.78[d]	nd[e] (br. s)	nd
7-OCH_3		3.24 (s)				

[a] Measured in acetone-d_6,

[b] Measured in $CDCl_3$,

[c, d, e] Assignments may be switched, nd = Not detected.

Table 3

^{13}C NMR Data for **7**–**12** (125 MHz)

position	**7**[a] δ_C (type)	**8**[a] δ_C (type)	**9**[a] δ_C (type)	**10**[a] δ_C (type)	**11**[a] δ_C (type)	**12**[b] δ_C (type)
1	166.6 (C)	166.7 (C)	166.8 (C)	166.6 (C)	166.6 (C)	165.4 (C)
2	118.7 (CH)	118.7 (CH)	118.7 (CH)	118.7 (CH)	119.5 (CH)	118.0 (CH)
3	158.3 (C)	158.5 (C)	158.7 (C)	159.5 (C)	156.9 (C)	156.3 (C)
4	32.2 (CH_2)	32.5 (CH_2)	31.9 (CH_2)	27.3 (CH_2)	29.4[c] (CH_2)	27.7 (CH_2)
5	35.4 (CH_2)	35.9 (CH_2)	33.2 (CH_2)	30.3[c] (CH_2)	35.6 (CH_2)	41.0 (CH_2)
6	76.6 (CH)	76.5 (CH)	76.7 (CH)	73.4 (CH)	73.5 (CH)	207.4 (C)
7	70.1 (CH)	79.6 (CH)	70.2 (CH)	70.0 (CH)	149.6 (CH)	41.5 (CH_2)
8	132.3 (CH)	129.2 (CH)	132.4 (CH)	131.4 (CH)	132.0 (CH)	119.7 (CH)
9	136.5 (CH)	140.3 (CH)	136.7 (CH)	139.2 (CH)	205.9[d] (C)	140.0 (CH)
10	29.3 (CH)	29.8[c] (CH)	29.9[c] (CH)	29.9[c] (CH)	36.4 (CH)	29.0 (CH)
11	32.0 (CH_2)	31.9 (CH_2)	32.2 (CH_2)	32.1 (CH_2)	29.4 (CH_2)	31.0 (CH_2)
12	32.9 (CH_2)	32.9 (CH_2)	35.4 (CH_2)	31.7 (CH_2)	32.4[c] (CH_2)	31.9 (CH_2)
13	62.3 (CH)	62.3 (CH)	62.6 (CH)	63.8 (CH)	63.1 (CH)	62.5 (CH)
14	36.6 (CH_2)	36.6 (CH_2)	36.9 (CH_2)	35.2 (CH_2)	36.3 (CH_2)	34.6 (CH_2)
15	68.2 (CH)	68.2 (CH)	68.1 (CH)	68.3 (CH)	67.9 (CH)	68.4 (CH)
16	32.0 (CH_2)	32.0 (CH_2)	32.6 (CH_2)	32.2 (CH_2)	36.5 (CH_2)	31.3 (CH_2)
17	97.6 (C)	97.7 (C)	97.4 (C)	98.1 (C)	97.7 (C)	97.3 (C)
18	63.4 (CH)	63.5 (CH)	64.0 (CH)	63.5 (CH)	63.6 (CH)	61.5 (CH)
19	28.9[c] (CH_2)	29.0[c] (CH_2)	29.4[c] (CH_2)	29.1[c] (CH_2)	29.0[c] (CH_2)	28.7 (CH_2)
20	173.9 (C)	174.0 (C)	174.2 (C)	173.9[d] (C)	174.0 (C)	174.9 (C)
21	25.4 (CH_3)	25.5 (CH_3)	25.5 (CH_3)	24.6 (CH_3)	25.1 (CH_3)	24.7 (CH_3)
22	23.1 (CH_3)	23.0 (CH_3)	23.2 (CH_3)	21.4 (CH_3)	19.6 (CH_3)	21.5 (CH_3)
OCH_3		56.5 (CH_3)				

[a] Measured in acetone-d_6,

[b] Measured in $CDCl_3$,

[c] Assignments from HMQC correlations (the spectra of **7**, **8**, **9**, **10** and **11** are available in Figures S11, S14, S17, S20 and S23, respectively),

[d] Assignments from HMBC correlations (the spectra of **10** and **11** are available in Figures S21 and S25).

Table 4

DFT Calculation Results of the Possible Isomers for **7** and **10**

	7		**10**	
Stereochem	**% Score**	**MAE (ppm)**	**% Score**	**MAE (ppm)**
6*S*,7*S*	95	2.1	86	2.1
6*R*,7*S*	95	2.4	95	1.7
6*S*,7*R*	86	2.6	77	3.0
6*R*,7*R*	86	2.5	86	2.2

Table 5

Bioassay Data for **1**–**12** and **7a**

compound	HCT-116 IC_{50} (μM)	MDA-MB-435 IC_{50} (μM)	Ratio MDA-MB-435/HCT116	MF disrupting Activity[a]
1	1.1	2.8 ± 0.3[b]	2.5	+
2	7.1	4.8 ± 0.1	0.7	+
3	38	17.0 ± 1.0	0.5	+
4	> 100	34.3 ± 5.4	< 0.3	−
5	49	29.7 ± 1.9	0.6	−
6	48	26.1 ± 1.0	0.5	−
7	0.48	2.1 ± 0.3	4.4	+
7a	5.1	7.9 ± 0.5	1.5	+
8	2.1	4.0 ± 0.5	1.9	+
9	5.5	> 50	> 9.1	−
10	> 53	11.9 ± 1.1	< 0.2	+
11	> 53	30.5 ± 2.4	< 0.6	−
12	0.92	1.0 ± 0.1	1.1	+

[a] The microfilament-disrupting effects were evaluated in rat aortic smooth muscle A10 cells, +: active at 5μM, −: inactive at 5μM.

[b] n = 3. IC_{50} values for HCT-116 and MDA-MB-435 were determined using trypane blue and SRB method, respectively.